

The BaR-SPOrt Experiment

M. Zannoni^{a,h}, S. Cortiglioni^b, G. Bernardi^b, E. Carretti^b, S. Cecchini^b, C. Macculi^b,
 E. Morelli^b, C. Sbarra^b, G. Ventura^b, L. Nicastro^c, J. Monari^d, M. Poloni^d, S. Poppi^d,
 V. Natale^e, M. Baralis^f, O. Peverini^f, R. Tascone^f, G. Virone^f, A. Boscaleri^g, E. Pascale^g,
 G. Boella^h, S. Bonometto^h, M. Gervasi^h, G. Sironi^h, M. Tucciⁱ, R. Nesti^j, R. Fabbri^k,
 P. de Bernardis^l, M. De Petris^l, S. Masi^l, M.V. Sazhin^m, E.N. Vinyajkinⁿ

^aCNR I.A.S.F.-Milano, ^bCNR I.A.S.F.-Bologna, ^cCNR I.A.S.F.-Palermo, Italy

^dCNR I.R.A.-Bologna, Italy, ^eCNR I.R.A.-Firenze, Italy

^fCNR I.R.I.T.I., Italy

^gCNR I.R.O.E., Italy

^hUniv. di Milano - Bicocca, Milano, Italy

ⁱInstituto de Fisica de Cantabria, Santander, Spain

^jOsservatorio Astrofisico di Arcetri, Firenze, Italy

^kUniv. di Firenze, Firenze, Italy

^lUniv. di Roma La Sapienza, Roma, Italy

^mMoscow State University-Moscow, ⁿN.I.R.F.I.-Novgorod, Russia

ABSTRACT

BaR-SPOrt (Balloon-borne Radiometers for Sky Polarisation Observations) is an experiment to measure the linearly polarized emission of sky patches at 32 and 90 GHz with sub-degree angular resolution. It is equipped with high sensitivity correlation polarimeters for simultaneous detection of both the U and Q stokes parameters of the incident radiation. On-axis telescope is used to observe angular scales where the expected polarization of the Cosmic Microwave Background (CMBP) peaks. This project shares most of the know-how and sophisticated technology developed for the SPOrt experiment onboard the International Space Station. The payload is designed to flight onboard long duration stratospheric balloons both in the Northern and Southern hemispheres where low foreground emission sky patches are accessible. Due to the weakness of the expected CMBP signal (in the range of μK), much care has been spent to optimize the instrument design with respect to the systematics generation, observing time efficiency and long term stability. In this contribution we present the instrument design, and first tests on some components of the 32 GHz radiometer.

Keywords: CMB, Polarization, Instrument, LDB

1. INTRODUCTION

The Cosmic Microwave Background (CMB) is the most sensitive tool to investigate the very high red-shift Universe.¹⁻⁵ Since its discovery in 1964,⁶ positive and precise results have been collected about the spectrum⁷⁻⁹ and the spatial distribution.¹⁰⁻¹² Current and future space missions like MAP* and Planck[†] are mainly devoted to the all-sky mapping of CMB small-scale anisotropies for which they will reach the highest sensitivities. A measure of the degree of residual polarization of the CMB, against its unique capability to solve the degeneracy among cosmological parameters that anisotropy alone is not able to remove,^{1,4,13,14} is not available yet. All the attempts to detect it produced only upper limits (see Table 1), since either the foreseen polarized component of

Further author information: (Send correspondence to M. Zannoni)

M. Zannoni: E-mail: zannoni@mi.iasf.cnr.it, Telephone: +39 02 23699331

Address: Istituto di Astrofisica Spaziale e Fisica Cosmica sezione di Milano, via Bassini 15, I-20133 Milano Italy

*<http://map.gsfc.nasa.gov/>

†<http://astro.estec.esa.nl/Planck/>

the CMB is definitely lower than the instrumental sensitivities or the contribution of the systematics dominates the final error budget. The most effective way to overcome such problems is to design dedicated experiments. One of them will be the space mission SPORt^{‡,15}. BaR-SPORt, a balloon experiment funded by ASI (Italian Space Agency), shares most of the know-how and technological development of the SPORt mission. While SPORt has for scientific target a nearly all sky polarization mapping at 22 and 32 GHz and a tentative detection of the CMBP at large angular scales ($> 7^\circ$) at 60 and 90 GHz, the goal of BaR-SPORt is to detect the CMBP in some low foreground regions with sub-degree angular resolution.

Resolution (deg)	Frequency (GHz)	Sky Coverage	Upper Limit	Reference
15	4	Scattered	300 mK	6
1.5 – 40	100 – 600	<i>GC</i>	3-0.3 mK	16
15	9.3	$\delta = +40^\circ$	1.8 mK	17
15	33	$+37^\circ \leq \delta \leq +63^\circ$	180 μ K	18
18'' – 160''	5	$\delta = +80^\circ$	4.2 mK - 120 μ K	19
1.2	26 – 36	<i>NCP</i>	30 μ K	20
1.4	26 – 36	<i>NCP</i>	18 μ K	21
7	33	<i>SCP</i>	267 μ K	22
6'	8.7	$\delta = -50^\circ$	16 μ K	23
0.24	90	<i>NCP</i>	11 μ K	24
7	26 – 36	$\delta = +43^\circ$	10 μ K	25

Table 1. Existing upper limits for the CMB linear polarization.

2. SCIENTIFIC MOTIVATIONS AND TARGETS

Detection of the extremely low signal level expected for the large scale polarization of the CMB (see Figure 1) needs a very stable environment. This is the reason why all-sky surveys can be only carried out in space where long observing time are feasible and very quiet and stable conditions exist. Ground-based and balloon-borne experiments can give scientific results observing small sky patches where they can reach sensitivities comparable with the expected level of polarization. As pointed out in Ref. 26, ground-based instruments operating in the millimeter domain are plagued by atmospheric emission which is the main source of spurious polarizations even in the best observing site like the Antarctic plateau. The instrumental polarization can correlate the unpolarized atmospheric signal producing offset, whose fluctuations can then degrade the expected sensitivity. A possible way out is to perform the observations from stratospheric altitude where the residual atmosphere contribution and its fluctuations are lower. The limited observing time (a long duration flight lasts for about two weeks - cf¹¹ but longer are feasible) reduces the typical targets to small sky patches ($\sim 4^\circ \times 4^\circ$ and smaller). On such portions of sky, sensitive polarization measurements at sub-degree scales, where the expected polarization peaks (see Figure 1 *left panel*), are reachable goals for instruments like BaR-SPORt, for which new state of the art millimeter devices have been developed. As shown in Figure 1, the expected *rms* polarization, P_{rms} , is maximum at small angular scales and is only weakly dependent on cosmological models. BaR-SPORt in the 90 GHz configuration, due to the beam-size of 0.2° , has the capability to detect CMBP (see Table 2) independently of the cosmological model. In the 32 GHz configuration, where the beam size is 0.4° ($P_{rms} \sim 2.1\mu$ K), BaR-SPORt will be able to improve the current upper limit on CMBP.

Both in the Northern and in the Southern hemisphere interesting sky patches are present. The ideal regions, from the CMB point of view, are the ones at high galactic latitude, far from local cirrus, where the foreground should be minimal. In the Southern sky, the patch observed by BOOMERanG¹¹ ($\alpha = 5^h$, $\delta = -45^\circ$) is the ideal target. Here the level of the foregrounds at 32 GHz, where the expected main contribution comes from synchrotron emission, can be evaluated from the Jonas²⁷ map at 2.3 GHz scaling it with a spectral index $\gamma = 3$ ($T^{synch} \propto \nu^{-3}$) and with a polarization fraction $P^{synch}/T^{synch} = 0.1$. We can derive a level of polarization

[‡]<http://sport.bo.iasf.cnr.it/>

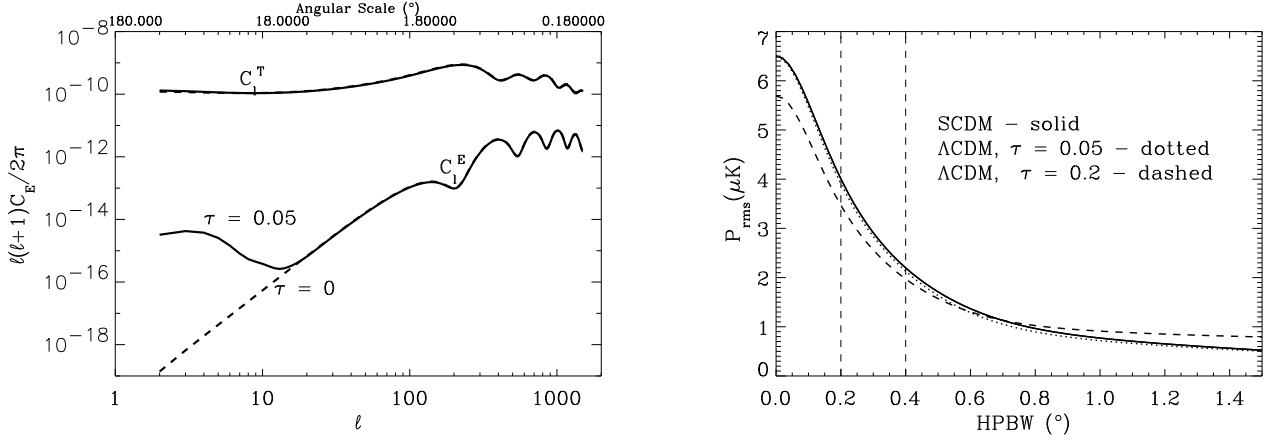


Figure 1. *Left:* anisotropy and E-mode power spectra. The expected polarized component of the CMB peaks in the sub-degree ($l \geq 100$) scales while the larger (degree) angular scales are more sensitive to the reionization scenarios. *Right:* the sky $P_{rms} = (\langle Q^2 \rangle + \langle U^2 \rangle)^{1/2}$ versus the beam width for different cosmological models. Vertical lines point out the BaR-SPOrt HPBWs at 32 and 90 GHz

$\Delta P < 1\mu\text{K}$ (making the synchrotron contribution at 90 GHz even lower). For the 90 GHz channel, where the dominant foreground contribution should come from dust, we find $\Delta P < 0.15\mu\text{K}$, starting from the DIRBE 240 μm map²⁸ and scaling the dust temperature²⁹ as $T^{dust} \propto \nu^{2.7} / (e^{h\nu/kT_D} - 1)$, using $P^{dust}/T^{dust} = 0.05$. In the Northern hemisphere for the region centered at $(\alpha = 10^h, \delta = +35^\circ)$ it is possible to derive $\Delta P < 0.3\mu\text{K}$ at 32 GHz and $\Delta P < 0.15\mu\text{K}$ at 90 GHz. For the latter we used again the DIRBE map, while for the former the data from the Reich³⁰ map at 1.4 GHz. In Figure 2 the aforementioned maps^{27, 28, 30} have been scaled as described for the evaluation of synchrotron and dust contribution respectively at the BaR-SPOrt frequencies; the selected patches both in the Northern and Southern sky are shown.

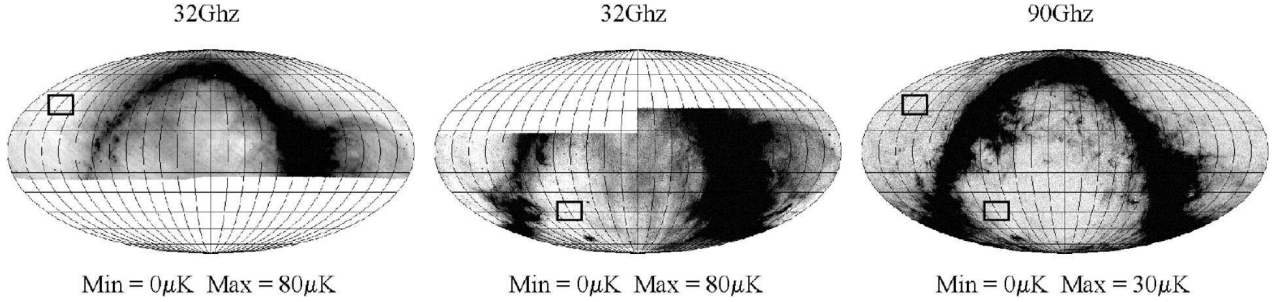


Figure 2. The three foreground maps computed radio^{27, 30} and far infra-red²⁸ data. The first two have been rescaled up to 32 GHz to evaluate the synchrotron component, while the last, related to the dust contribution, has been scaled down to 90 GHz. The two target patches have been superimposed.

From a logistical point of view, both patches are effectively observable with Long Duration Balloon (LDB) flights. The one in the Southern Sky is accessible from Antarctica, while the one in the Northern hemisphere can be observed with a flight launched from the available facilities both in Norway³¹ and in Sweden.³² Simulations are under development to optimize the patch dimension, scanning speed and path for maximizing the final full patch sensitivity. Expected raw sensitivities are reported in Table 2.

Frequencies (GHz)	Bandwidth	Beamsize	σ_{1s} [mKs ^{1/2}]	$\sigma_{pix}^{2wfl[4wfl]}(\mu\text{K})$	$\sigma_{prms}^{2wfl[4wfl]}(\mu\text{K})$
32	10%	0.4°	0.5	4.5 [3.2]	3.0 [2.0] (2 σ up. lim.)
90	20%	0.2°	0.5	4.5 [3.2]	0.7 [0.4]

Table 2. BaR-SPOrt expected sensitivities: σ_{1s} is the instantaneous sensitivity, $\sigma_{pix}^{2wfl[4wfl]}$ is the pixel sensitivity considering a 2 [4] week flight and 100 pixel patch; $\sigma_{prms}^{2wfl[4wfl]}$ is the corresponding sensitivity on P_{rms} . Due to the low P_{rms} foreseen at 32 GHz (2.1 μK against 4.0 μK at 90 GHz) the low frequency channel is expected to provide upper limits.

3. THE INSTRUMENT

The BaR-SPOrt payloads house correlation microwave polarimeters (see Figures 3 and 4) for direct measurement of the Q and U Stokes parameters with HPBW=0.4° at 32 GHz and 0.2° at 90 GHz. 1.8 m and 1.2 m on axis Cassegrain configurations (for 32 and 90 GHz, respectively) are adopted to meet the very stringent requirements of extremely low spurious polarization (fractions of μK) necessary for such measurements (for a general discussion see Ref. 26). The detection of signals as low as those expected from CMB polarization implies the use of extremely sensitive and stable radiometers. BaR-SPOrt has been designed to minimize instrumental effects and to reduce $1/f$ noise, thereby increasing the long term stability. Great care has been taken to realize the antenna system keeping under control the spurious polarization. The undesirable consequences of gain fluctuations are greatly reduced by the correlation technique, while residual instabilities are recovered using destriping data analysis,^{33–37} which requires the radiometer to be stable only over a single scan period (the scanning time of BaR-SPOrt is of the order of 1 minute).

The main instrumental characteristics are:

- direct amplification architecture: no down conversion to avoid possible additional phase error;
- on axis low cross-polarization optics providing HPBW of 0.4° (0.2°) at 32 GHz (90 GHz);
- correlation unit based on a custom design waveguide Hybrid Phase Discriminator (HPD), capable of rejecting the unpolarized component better than 30 dB^{38,39} and a phase modulation (lock-in system) providing > 60 dB of total rejection to the unpolarized component;
- custom design Orthomode Transducer (OMT) with high isolation between channels (> 60 dB) to limit contaminations from the unpolarized component;
- a cryostat (see Figure 9) to cool down to $T < (80.0 \pm 0.1)$ K the Low Noise Amplifiers, the circulators, the polarizer and the OMT by a closed loop cryocooler. The horn is kept, in the present design, at ≈ 300 K, but might be cooled as well. A thermal shield stabilized at temperature $T \cong (300.0 \pm 0.1)$ K, is adopted to increase the thermal stability of warm parts;
- custom design internal calibrator to inject reference polarized signals.⁴⁰

The antenna system collects the incoming radiation and transforms, by means of the polarizer, the linearly polarized components (E_x, E_y) of the electric field into the circularly ones (E_R, E_L) which are picked up by the Ortho-Mode Transducer⁴¹ (see Figures 4).

The lock-in detection is obtained by modulation ($0 - \pi$ phase shift) of one of the signals of the two chains just after the first stage of amplification (LNA) and then by synchronous detection in the back-end. Just before correlation, but inside the Hybrid Phase Discriminator, a fraction of the signal is picked-up and fed into two total power detectors to record the sky temperature and for monitoring of the system temperature too. The heart of the correlation unit is the custom design HPD³⁸ that processes the signal in order to have four outputs proportional to:

$$\vec{E}_R - \vec{E}_L \quad \vec{E}_R + \vec{E}_L \quad \vec{E}_R + j\vec{E}_L \quad \vec{E}_R - j\vec{E}_L \quad (1)$$

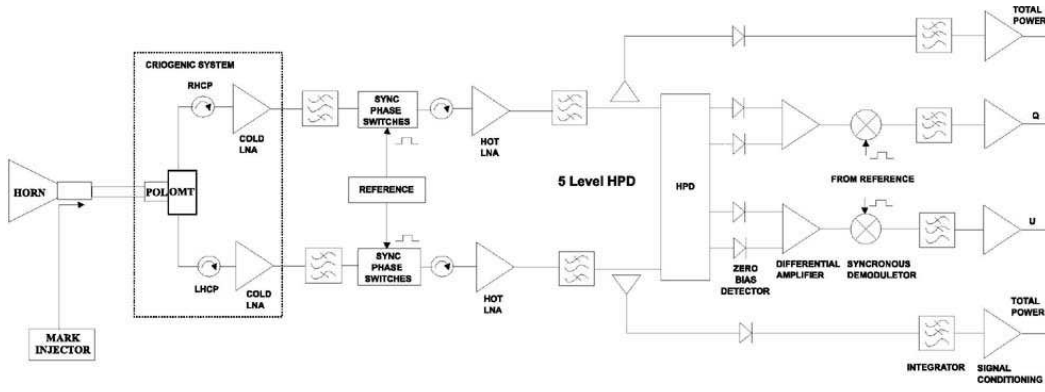


Figure 3. Block diagram of the BaR-SPOrt radiometers.

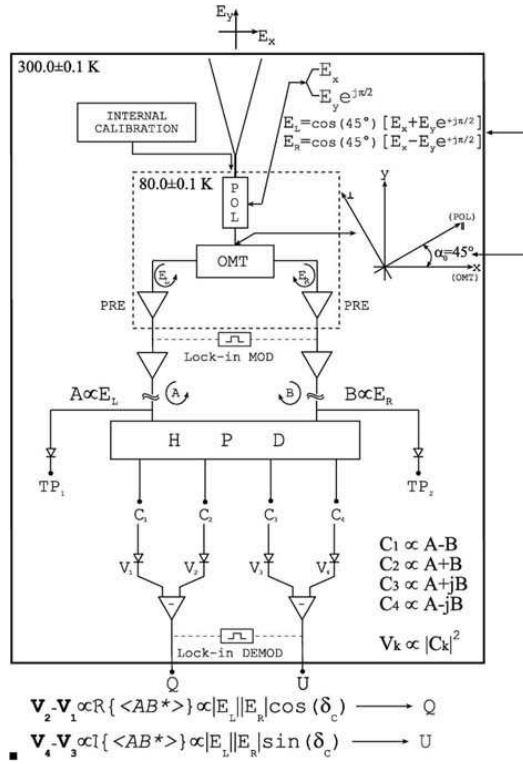


Figure 4. Scheme of the radiometers with the propagation of the fields collected by the feed horn.

After square law detection the four HPD outputs are:

$$\begin{aligned}
 V_1 &\propto [|\vec{E}_L|^2 + |\vec{E}_R|^2 - 2\Re(\vec{E}_L \cdot \vec{E}_R^*)] \\
 V_2 &\propto [|\vec{E}_L|^2 + |\vec{E}_R|^2 + 2\Re(\vec{E}_L \cdot \vec{E}_R^*)] \\
 V_3 &\propto [|\vec{E}_L|^2 + |\vec{E}_R|^2 + 2\Im(\vec{E}_L \cdot \vec{E}_R^*)] \\
 V_4 &\propto [|\vec{E}_L|^2 + |\vec{E}_R|^2 - 2\Im(\vec{E}_L \cdot \vec{E}_R^*)]
 \end{aligned} \tag{2}$$

which are properly differentiated to get as final outputs the two quantities:

$$\begin{aligned} V_2 - V_1 &\propto |\vec{E}_L| |\vec{E}_R| \cos(\delta_c) \longrightarrow Q \\ V_4 - V_3 &\propto |\vec{E}_L| |\vec{E}_R| \sin(\delta_c) \longrightarrow U \end{aligned} \quad (3)$$

where δ_c is the phase delay between the two (L&R) circular components of the electric field. After integration, these provide time averaged values proportional to the Q and U Stokes parameters.

4. PRELIMINARY PERFORMANCE EVALUATION OF SOME CUSTOM DEVELOPED COMPONENTS OF THE 32 GHZ RADIOMETER

The tininess of the CMBP signal translates in very stringent requirements of some critical components of the radiometer. These are mainly the ones where the polarizations propagate together^{26,42}: in the front-end we find, after the feed horn, the Reference Marker Injector (the calibrator), the Polarizer and the OrthoMode Transducer while in the back-end the Hybrid Phase Discriminator. Here we report only about the devices in the front-end, the performances of the HPD being already evaluated in Ref. 38,39.

The Reference Marker Injector is crucial in experiments like BaR-SPOrt where external devices like wire grids or diplexers to periodically feed the radiometer with known polarization signals are difficult, if not impossible, to be used. We have realized a marker injector⁴⁰ (Figure 5 **left**) able to inject polarized signals with three different polarization angles (nominally $\frac{\pi}{8}, \frac{\pi}{8} \pm \frac{\pi}{4}$). The S parameters of this device are reported in Figure 6. The coupling factor can be adjusted simply changing the length of the pins spilling the radiation (central panel). This is very important both to reduce and control the amplitude of the mark, produced by a noise generator, and not to degrade the polarization status of the travelling sky signal. The last panel shows the insertion loss of the device without silver coating: the very low S_{21} parameter (~ -0.025 dB) will be even lower with the foreseen silver plating.



Figure 5. **Left image** shows the marker-injector. The device has 8 points where to inject polarized reference signals. Only three of them are fed, the remaining are for symmetry reasons. See text for a more detailed description. **Central image** shows the Iris Polarizer realized in circular waveguide. **Right image** shows the high isolation OrthoMode Transducer.

With these reference signals periodically injected, adopting the calibration technique described in Ref. 40, it is possible to fully reconstruct the transfer matrixes of the instrument.

After the marker injector and a waveguide thermal choke, there is the cold part of the radiometer housing the polarizer, the OMT and the LNAs. The polarizer, visible in the central panel of Figure 5, is realized inserting some irises in a circular waveguide. Great care has been taken to keep the transmission coefficients for both polarizations extremely similar: in the device realized their mean and maximum ratio are 0.0047 dB and 0.01 dB respectively. Since a difference in the S_{21} parameters means an offset generation, their equalizations was a key-point in the device design. The $\frac{\pi}{2}$ phase difference between the polarizations is constant too. As a matter of fact it is possible to show that a not constant phase difference inside the integration bandwidth translates into depolarization. The BaR-SPOrt custom polarizer keeps this difference within 0.48° (with a mean value of 89.96°). The S_{11} parameters are always below -50 dB all over the bandwidth (Figure 7).

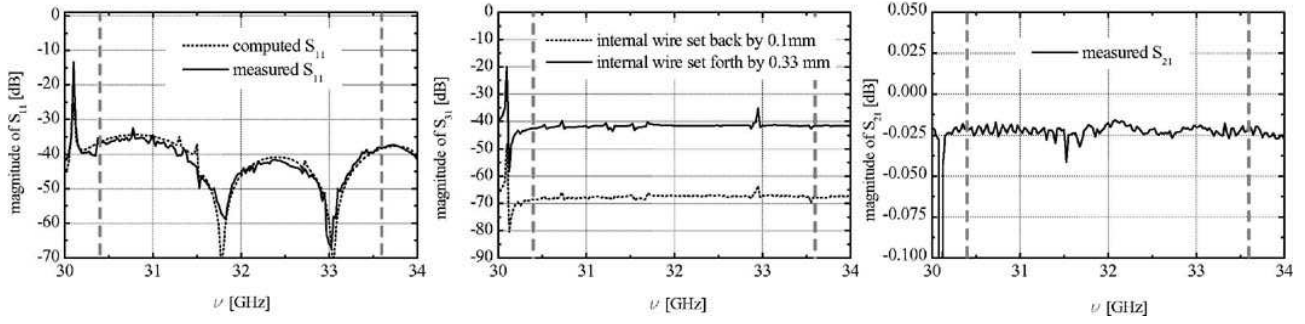


Figure 6. S parameters for the *marker injector*: dotted lines are for simulations while solid ones are for experimental data from the real device. Vertical dashed lines show the BaR-SPOrt bandwidth. **Left panel** shows the S_{11} parameter. **Central panel** shows two different coupling factors of reference polarized signals: adjusting the position of the injector pins which feed the reference signals it is possible to fine tune the coupling factor. **Right panel** shows the overall insertion loss of the device. The measured data are for an aluminum device before silver plating.

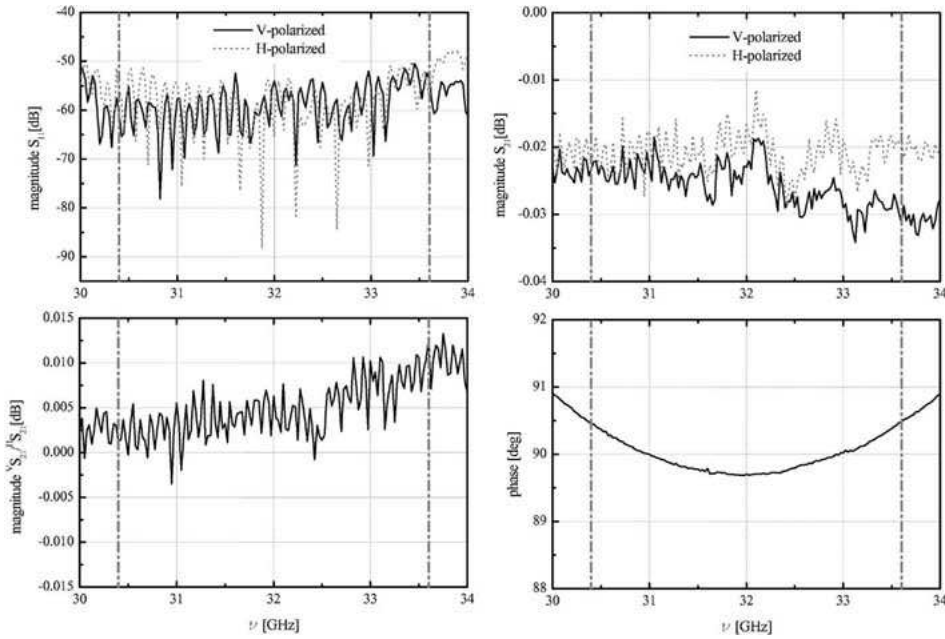


Figure 7. The characteristic of the polarizer. **Up left panel** shows the reflection coefficient at the input port of the polarizer. **Up right panel** reports the transmission coefficients (S_{21}) of the two perpendicular polarizations. **Down left panel** shows the difference between the two S_{21} parameters. **Down right panel** is the phase difference between the two polarizations. Vertical dashed lines show the BaR-SPOrt bandwidth.

The OMT is the device devoted to the polarization separation. Its ability to correctly separate the vertical from the horizontal polarization impacts on the final sensitivity of the experiment.²⁶ The cross-talk and isolation between the two polarizations measure the quality of this device. In the BaR-SPOrt OMT we reached an extremely low polarization contamination, both cross-talks and isolation being always well below -60 dB (Figure 8).

Since the BaR-SPOrt performances strongly depend on the thermal stability, particular care has been taken in the thermal design (see Figure 9). The cooling system of BaR-SPOrt is based on a mechanical Stirling

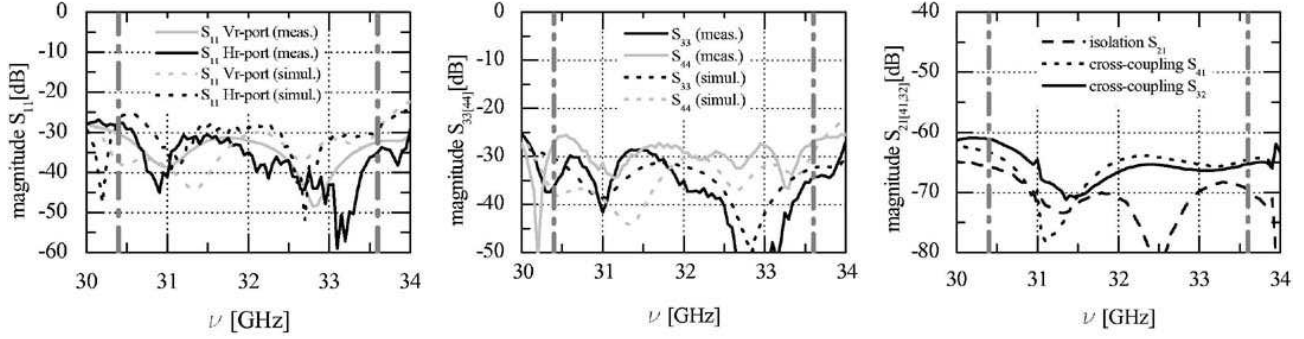


Figure 8. S parameters for the *OMT*: dotted lines are for simulations while solid ones are for experimental data from the real device. Vertical dashed lines show the BaR-SPOrt bandwidth. **Left panel** shows the S_{11} parameters of the rectangular output ports. **Central panel** shows the reflection coefficients for the square input port. **Right panel** shows both the isolation and the cross-coupling: S_{21} measures the signal arriving in the horizontal port when the vertical one is fed and the square input is closed with a matched load. S_{41} measures the horizontal polarization contaminating the vertical one and S_{32} vice-versa.

cryocooler[§] with closed loop control. Such cryogenerator can cool the cold part of the radiometer down to 80 K with stability better than 0.1 K. A laboratory dry run on the cooler lasted about 8 days, has shown a very good stability. Without any thermal control over the environment (the laboratory) and any mass with high thermal inertia anchored to the cold finger, the cooler was extremely stable (see Figure 10), showing the high effectiveness of the controller PID algorithm (for some more preliminary results on the cooling system see Macculi *et al.*⁴³).

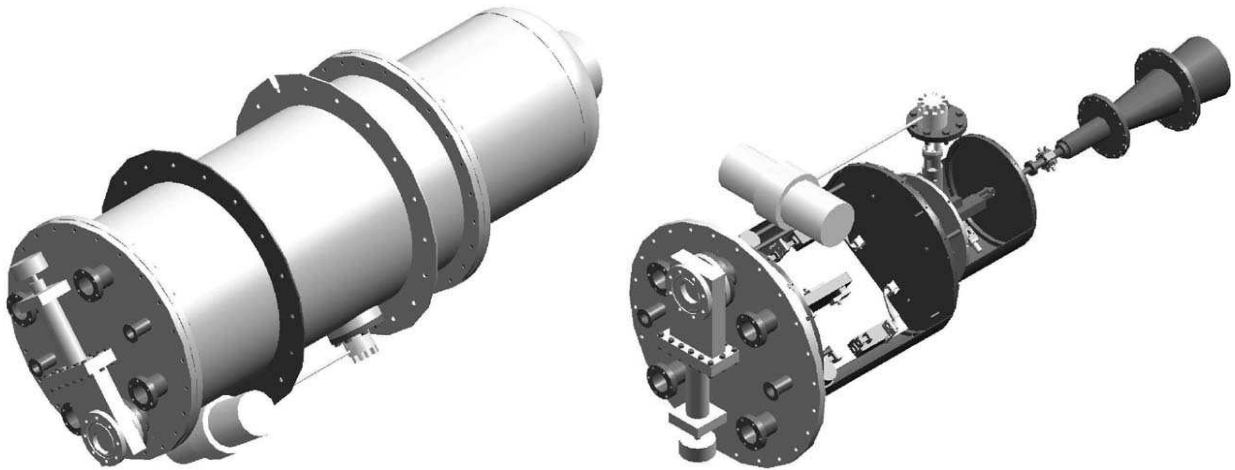


Figure 9. The cryostat (left) housing the 32 GHz radiometer of BaR-SPOrt with the closed loop cryocooler visible in the foreground. The radiometer inside the cryostat (right).

5. CONCLUSIONS

The BaR-SPOrt experiment is one of the first instruments with the potentiality to measure, in its 90 GHz configuration, the CMB polarization on sub-degree angular scale. When operated in the 32 GHz configuration, even if probably not enough sensitive for a CMBP detection, it will permit to refine the existing upper limit

[§]Leybold model Polar SC-7 COM

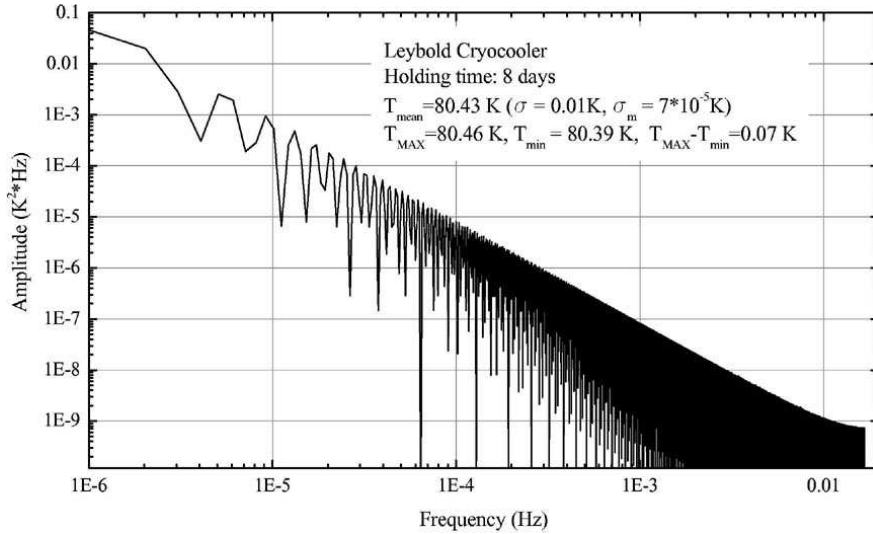


Figure 10. Power Spectrum of the Leybold cryocooler computed for 8 days of dry run. The cooler has a very good stability thanks to the PID algorithm governing the heat sink temperature.

on the CMBP and will give data extremely important for the studies of the polarized galactic foregrounds, in the light of the BaR-SPOrt 90 GHz flight and the incoming CMB space missions (SPOrt and, later, Planck). BaR-SPOrt represents also a very good opportunity to test in operative conditions state of the art technological solutions to be used in the SPOrt mission.

ACKNOWLEDGMENTS

Authors wish to thank A.S.I. (Italian Space Agency) for the full support to BaR-SPOrt and P.N.R.A. (National Project for Research in Antarctica) for its relevant contribution. E.N.V. and M.V.S. are grateful to C.N.R. (National Council for Research) for supporting their collaboration within the C.N.R.-R.A.S (Russian Academy of Science) agreement. We acknowledge use of CMBFAST and HEALPix packages for performing our analysis.

REFERENCES

1. V. A. Rubakov, M. V. Sazhin, and A. V. Veryaskin, “Graviton creation in the inflationary universe and the grand unification scale,” *Physics Letters B*, 1982.
2. A. D. Dolgov, M. V. Sazhin, and Y. B. Zeldovich, *Basics of modern cosmology*, Gif-sur-Yvette, France, Editions Frontieres, 1990, 251 p. Translation., 1990.
3. G. Jungman, M. Kamionkowski, A. Kosowsky, and D. N. Spergel, “Cosmological-parameter determination with microwave background maps,” *Physical Review D* **54**, pp. 1332–1344, July 1996.
4. M. Zaldarriaga, D. N. Spergel, and U. Seljak, “Microwave Background Constraints on Cosmological Parameters,” *Astrophysical Journal* **488**, pp. 1+, Oct. 1997.
5. G. Efstathiou and J. R. Bond, “Cosmic confusion: degeneracies among cosmological parameters derived from measurements of microwave background anisotropies,” *Monthly Notices of the Royal Astronomical Society* **304**, pp. 75–97, Mar. 1999.
6. A. A. Penzias and R. W. Wilson, “A Measurement of Excess Antenna Temperature at 4080 Mc/s.,” *Astrophysical Journal* **142**, pp. 419–421, July 1965.
7. G. F. Smoot, G. de Amici, S. D. Friedman, C. Witebsky, G. Sironi, G. Bonelli, N. Mandolesi, S. Cortiglioni, G. Morigi, and R. B. Partridge, “Low-frequency measurements of the cosmic background radiation spectrum,” *Astrophysical Journal Letters* **291**, pp. L23–L27, Apr. 1985.

8. D. J. Fixsen, E. S. Cheng, J. M. Gales, J. C. Mather, R. A. Shafer, and E. L. Wright, "The Cosmic Microwave Background Spectrum from the Full COBE FIRAS Data Set," *Astrophysical Journal* **473**, pp. 576+, Dec. 1996.
9. M. Zannoni, G. Boella, G. Bonelli, F. Cavaliere, M. Gervasi, A. Lagostina, A. Passerini, G. Sironi, and A. Vaccari, "TRIS Experiment: A Search for Spectral Distortions in the CMB Spectrum Close to 1 GHz," in *AIP Conf. Proc. 476: 3K cosmology*, pp. 165+, 1999.
10. C. L. Bennett, A. J. Banday, K. M. Gorski, G. Hinshaw, P. Jackson, P. Keegstra, A. Kogut, G. F. Smoot, D. T. Wilkinson, and E. L. Wright, "Four-Year COBE DMR Cosmic Microwave Background Observations: Maps and Basic Results," *Astrophysical Journal Letters* **464**, pp. L1–+, June 1996.
11. P. de Bernardis, P. A. R. Ade, J. J. Bock, J. R. Bond, J. Borrill, A. Boscaleri, K. Coble, B. P. Crill, G. De Gasperis, P. C. Farese, P. G. Ferreira, K. Ganga, M. Giacometti, E. Hivon, V. V. Hristov, A. Iacoangeli, A. H. Jaffe, A. E. Lange, L. Martinis, S. Masi, P. V. Mason, P. D. Mauskopf, A. Melchiorri, L. Miglio, T. Montroy, C. B. Netterfield, E. Pascale, F. Piacentini, D. Pogosyan, S. Prunet, S. Rao, G. Romeo, J. E. Ruhl, F. Scaramuzzi, D. Sforna, and N. Vittorio, "A flat Universe from high-resolution maps of the cosmic microwave background radiation," *Nature* **404**, pp. 955–959, Apr. 2000.
12. S. Hanany, P. Ade, A. Balbi, J. Bock, J. Borrill, A. Boscaleri, P. de Bernardis, P. G. Ferreira, V. V. Hristov, A. H. Jaffe, A. E. Lange, A. T. Lee, P. D. Mauskopf, C. B. Netterfield, S. Oh, E. Pascale, B. Rabbii, P. L. Richards, G. F. Smoot, R. Stompor, C. D. Winant, and J. H. P. Wu, "MAXIMA-1: A Measurement of the Cosmic Microwave Background Anisotropy on Angular Scales of 10° – 5° ," *Astrophysical Journal Letters* **545**, pp. L5–L9, Dec. 2000.
13. M. V. Sazhin and V. A. Korolev, "Polarization of the Unresolved-Source Microwave Background," *Soviet Astronomy Letters* **11**, pp. 204–+, July 1985.
14. M. V. Sazhin and N. Benitez, "Detecting gravitational waves via the Cosmic Microwave Background Polarization," *Astrophysical Letters and Communications* **32**, pp. 105–+, 1995.
15. E. Carretti, M. Baralis, G. Bernardi, G. Boella, S. Bonometto, M. Bruscoli, S. Cecchini, S. Cortiglioni, R. Fabbri, M. Gervasi, M. Gervasi, C. Macculi, J. Monari, K. Ng, L. Nicastro, A. Orfei, O. Peverini, S. Poppi, V. Razin, M. Sazhin, C. Sbarra, G. Sironi, I. Strukov, R. Tascone, M. Tucci, E. Vinyaikin, and M. Zannoni, "The SPORt Experiment," in *AIP Conf. Proc. 609: Astrophysical Polarized Backgrounds*, pp. 109+, 2002.
16. N. Caderni, R. Fabbri, B. Melchiorri, F. Melchiorri, and V. Natale, "Polarization of the microwave background radiation. I - Anisotropic cosmological expansion and evolution of the polarization states. II - an infrared survey of the sky," *Physical Review D* **17**, pp. 1901–1918, Apr. 1978.
17. G. P. Nanos, "Polarization of the blackbody radiation at 3.2 centimeters," *Astrophysical Journal* **232**, pp. 341–347, Sept. 1979.
18. P. M. Lubin and G. F. Smoot, "Polarization of the cosmic background radiation," *Astrophysical Journal* **245**, pp. 1–17, Apr. 1981.
19. R. B. Partridge, J. Nowakowski, and H. M. Martin, "Linear polarized fluctuations in the cosmic microwave background," *Nature* **331**, pp. 146+, Jan. 1988.
20. E. J. Wollack, N. C. Jarosik, C. B. Netterfield, L. A. Page, and D. Wilkinson, "A Measurement of the Anisotropy in the Cosmic Microwave Background Radiation at Degree Angular Scales," *Astrophysical Journal Letters* **419**, pp. L49–+, Dec. 1993.
21. C. B. Netterfield, N. Jarosik, L. Page, D. Wilkinson, and E. Wollack, "The anisotropy in the cosmic microwave background at degree angular scales," *Astrophysical Journal Letters* **445**, pp. L69–L72, June 1995.
22. G. Sironi, G. Boella, G. Bonelli, L. Brunetti, F. Cavaliere, M. Gervasi, G. Giardino, and A. Passerini, "A 33 GHz polarimeter for observations of the Cosmic Microwave Background," *New Astronomy* **3**, pp. 1–13, Nov. 1997.
23. R. Subrahmanyan, M. J. Kesteven, R. D. Ekers, M. Sinclair, and J. Silk, "An Australia Telescope survey for CMB anisotropies," *Monthly Notices of the Royal Astronomical Society* **315**, pp. 808–822, July 2000.

24. M. M. Hedman, D. Barkats, J. O. Gundersen, J. J. McMahon, S. T. Staggs, and B. Winstein, "New Limits on the Polarized Anisotropy of the Cosmic Microwave Background at Subdegree Angular Scales," *Astrophysical Journal Letters* **573**, pp. L73–LL76, July 2002.
25. B. G. Keating, C. W. O'Dell, A. de Oliveira-Costa, S. Klavikowski, N. Stebor, L. Piccirillo, M. Tegmark, and P. T. Timbie, "A Limit on the Large Angular Scale Polarization of the Cosmic Microwave Background," *Astrophysical Journal Letters* **560**, pp. L1–L4, Oct. 2001.
26. E. Carretti, R. Tascone, S. Cortiglioni, J. Monari, and M. Orsini, "Limits due to instrumental polarisation in CMB experiments at microwave wavelengths," *New Astronomy* **6**, pp. 173–187, May 2001.
27. J. L. Jonas, E. E. Baart, and G. D. Nicolson, "The Rhodes/HartRAO 2326-MHz radio continuum survey," *Monthly Notices of the Royal Astronomical Society* **297**, pp. 977–989, July 1998.
28. M. G. Hauser, R. G. Arendt, T. Kelsall, E. Dwek, N. Odegard, J. L. Weiland, H. T. Freudenreich, W. T. Reach, R. F. Silverberg, S. H. Moseley, Y. C. Pei, P. Lubin, J. C. Mather, R. A. Shafer, G. F. Smoot, R. Weiss, D. T. Wilkinson, and E. L. Wright, "The COBE Diffuse Infrared Background Experiment Search for the Cosmic Infrared Background. I. Limits and Detections," *Astrophysical Journal* **508**, pp. 25–43, Nov. 1998.
29. M. Tegmark, D. J. Eisenstein, W. Hu, and A. de Oliveira-Costa, "Foregrounds and Forecasts for the Cosmic Microwave Background," *Astrophysical Journal* **530**, pp. 133–165, Feb. 2000.
30. P. Reich and W. Reich, "A radio continuum survey of the northern sky at 1420 MHz. II," *Astronomy and Astrophysics Supplement* **63**, pp. 205–288, Feb. 1986.
31. K. Bøen, "Scientific Ballons from Svalbard," in *AIP Conf. Proc. 609: Astrophysical Polarized Backgrounds*, pp. 243+, 2002.
32. P. Baldemar and O. Widell, "The Esrange Facility in Northern Sweden—Your Partner for Successful Aerospace Operations," in *AIP Conf. Proc. 609: Astrophysical Polarized Backgrounds*, pp. 239+, 2002.
33. C. Sbarra, E. Carretti, S. Cortiglioni, M. Zannoni, R. Fabbri, C. Macculi, and M. Tucci, "A Destriping Technique for SPORt Polarization Data," in *AIP Conf. Proc. 609: Astrophysical Polarized Backgrounds*, pp. 193+, 2002.
34. J. Delabrouille, "Analysis of the accuracy of a destriping method for future cosmic microwave background mapping with the PLANCK SURVEYOR satellite," *Astronomy and Astrophysics Supplement* **127**, pp. 555–567, Feb. 1998.
35. E. L. Wright, "Scanning and Mapping Strategies for CMB Experiments. Paper presented at the IAS CMB Data Analysis Workshop in Princeton on 22 Nov 96," in *astro-ph/9612006*, 1996.
36. C. Sbarra and et al., "in preparation,"
37. B. Revenu, A. Kim, R. Ansari, F. Couchot, J. Delabrouille, and J. Kaplan, "Destriping of polarized data in a CMB mission with a circular scanning strategy," *Astronomy and Astrophysics Supplement* **142**, pp. 499–509, Mar. 2000.
38. R. Tascone, D. Trinchero, M. Baralis, O. Peverini, A. Olivieri, E. Carretti, and S. Cortiglioni, "Millimeter Wave Passive Devices for Measurements of the Polarized Sky Emission," in *AIP Conf. Proc. 616: Experimental Cosmology at Millimetre Wavelengths*, pp. 150+, 2002.
39. O. Peverini, M. Baralis, R. Tascone, D. Trinchero, A. Olivieri, E. Carretti, and S. Cortiglioni, "Millimeter Wave Passive Components for Polarization Measurements," in *AIP Conf. Proc. 609: Astrophysical Polarized Backgrounds*, pp. 177+, 2002.
40. M. Baralis, O. Peverini, R. Tascone, D. Trinchero, V. Niculae, A. Olivieri, E. Carretti, S. Cortiglioni, C. Macculi, J. Monari, A. Orfei, G. Sironi, and M. Zannoni, "Calibration Techniques and Devices for Correlation Radiometers Used in Polarization Measurements," in *AIP Conf. Proc. 609: Astrophysical Polarized Backgrounds*, pp. 257+, 2002.
41. C. Macculi, G. Bernardi, E. Carretti, S. Cecchini, S. M. E. Cortiglioni, C. Sbarra, V. G., J. Monari, S. Poppi, G. Boella, S. Bonometto, M. Gervasi, G. Sironi, M. Tucci, M. Zannoni, M. Baralis, O. Peverini, R. Tascone, R. Fabbri, V. Natale, M. Bruscoli, A. Boscaleri, E. Pascale, and L. Nicastro, "BaR-SPORt: a technical overview," in *AIP Conf. Proc. 616: Experimental Cosmology at Millimetre Wavelengths*, pp. 145+, 2002.

42. E. Carretti and et al., "SPOrt: an Experiment Aimed at Measuring the Large Scale Cosmic Microwave Background Polarization," *this volume* .
43. C. Macculi and M. Zannoni, "Thermal Design and Preliminary Performance Evaluation of the Cooling System for BaR-SPOrt," in *AIP Conf. Proc. 609: Astrophysical Polarized Backgrounds*, pp. 275+, 2002.